

## MIT Open Access Articles

*Domain wall induced magnetoresistance in  
a superconductor/ferromagnet nanowire*

The MIT Faculty has made this article openly available. **Please share**  
how this access benefits you. Your story matters.

**Citation:** Miao, G. X., M. D. Mascaró, C. H. Nam, C. A. Ross, and J. S. Moodera. "Domain wall induced magnetoresistance in a superconductor/ferromagnet nanowire." *Applied Physics Letters* 99, no. 3 (2011): 032501. © 2011 American Institute of Physics

**As Published:** <http://dx.doi.org/10.1063/1.3610947>

**Publisher:** American Institute of Physics (AIP)

**Persistent URL:** <http://hdl.handle.net/1721.1/79742>

**Version:** Final published version: final published article, as it appeared in a journal, conference proceedings, or other formally published context

**Terms of Use:** Article is made available in accordance with the publisher's policy and may be subject to US copyright law. Please refer to the publisher's site for terms of use.



## Domain wall induced magnetoresistance in a superconductor/ferromagnet nanowire

G. X. Miao, M. D. Mascaró, C. H. Nam, C. A. Ross, and J. S. Moodera

Citation: *Appl. Phys. Lett.* **99**, 032501 (2011); doi: 10.1063/1.3610947

View online: <http://dx.doi.org/10.1063/1.3610947>

View Table of Contents: <http://apl.aip.org/resource/1/APPLAB/v99/i3>

Published by the AIP Publishing LLC.

---

### Additional information on *Appl. Phys. Lett.*

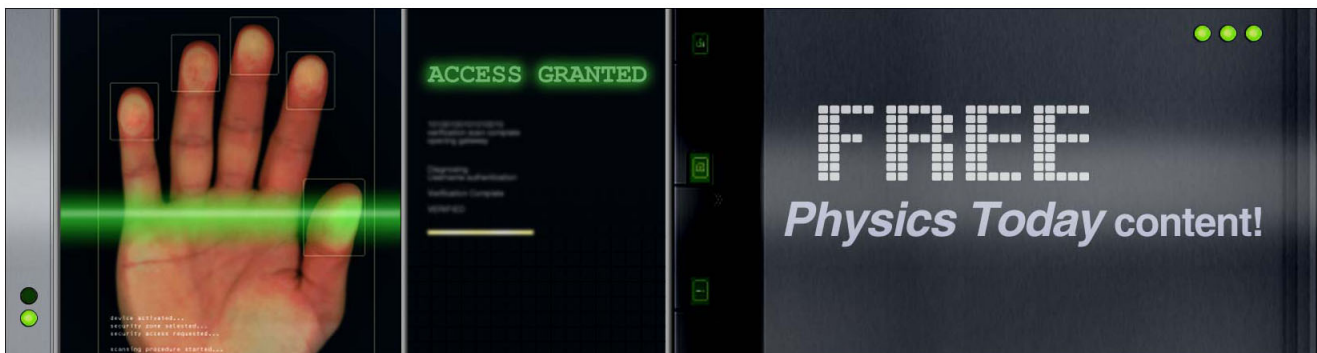
Journal Homepage: <http://apl.aip.org/>

Journal Information: [http://apl.aip.org/about/about\\_the\\_journal](http://apl.aip.org/about/about_the_journal)

Top downloads: [http://apl.aip.org/features/most\\_downloaded](http://apl.aip.org/features/most_downloaded)

Information for Authors: <http://apl.aip.org/authors>

## ADVERTISEMENT



## Domain wall induced magnetoresistance in a superconductor/ferromagnet nanowire

G. X. Miao,<sup>1,a)</sup> M. D. Mascaró,<sup>2</sup> C. H. Nam,<sup>2</sup> C. A. Ross,<sup>2</sup> and J. S. Moodera<sup>1</sup>

<sup>1</sup>Francis Bitter Magnet Lab, Massachusetts Institute of Technology, Cambridge, Massachusetts 02139, USA

<sup>2</sup>Department of Materials Science and Engineering, Massachusetts Institute of Technology, Cambridge, Massachusetts 02139, USA

(Received 14 April 2011; accepted 29 April 2011; published online 18 July 2011)

In a nanowire consisting of a ferromagnet/insulator/superconductor multilayer structure, the superconductivity is shown to depend strongly on the configuration of the magnetic domain walls in the neighboring ferromagnetic layer, yielding a high magnetoresistance within a temperature range near the superconducting transition temperature  $T_C$ . Micromagnetic simulations confirmed that out-of-plane stray magnetic fields from uncompensated magnetic poles play a dominant role in inducing magnetoresistance in this particular system. © 2011 American Institute of Physics.

[doi:10.1063/1.3610947]

A superconductor shows great tunability in its behavior when placed in the vicinity of a ferromagnet and thus has been of intense scientific interest for decades. The two phenomena, ferromagnetism (FM) and superconductivity (SC), are usually incompatible: in a ferromagnetic material, adjacent electron spins align parallel to each other, while in a superconductor, the spins are aligned antiparallel in order to form Cooper pairs. The competition between these two types of spin ordering provides the opportunity to create devices with unique functionalities, for examples to achieve very large magnetoresistance (MR) in superconducting spin valves,<sup>1,2</sup> to establish quantum communication using Andreev entanglement,<sup>3,4</sup> or to create and braid non-abelian Majorana fermions on magnetic proximity driven  $p_x + ip_y$  superconductor surfaces.<sup>5,6</sup>

In a ferromagnet, the magnetic configuration can be easily tuned with an external magnetic field, making magnetic devices suitable for memory and logic applications. On the other hand, local control of superconductivity is less straightforward, usually involving more complicated approaches such as an interaction with a ferromagnet. The influence of a ferromagnet on an adjacent superconductor can be three-fold. When the materials are sufficiently close, Cooper pairs from the superconductor can penetrate into the ferromagnet and experience the exchange field. This proximity effect<sup>7,8</sup> arises from direct electron-electron correlations and is extremely strong yet short ranged, typically extending no more than a couple of coherence lengths. Conversely, spin polarized carriers from the ferromagnet can also penetrate the superconductor and induce a finite magnetization inside, which results in a net imbalance between the two spin channels and thus suppresses superconductivity. The third influence of the ferromagnet is indirect but longer range, originating from the stray magnetic fields generated around magnetic poles<sup>9</sup> which tend to locally suppress superconductivity due to the competition between the Cooper pairing energy and the Zeeman energy.

Superconducting spin valve structures<sup>1,2</sup> consisting of superlattices of ferromagnets and superconductors can be constructed, and extremely large magnetoresistance has been

obtained and attributed to proximity effects<sup>10–13</sup> and spin accumulation,<sup>14–16</sup> as well as to nucleation of magnetic domain walls.<sup>17–21</sup> In this letter, we demonstrate the controllable creation and motion of magnetic domain walls in narrow magnetic stripes and study their influence on a neighboring superconductor. We see that such bilayer superconducting spin valves respond to the formation of domain walls by generating a very large *positive* magnetoresistance along the wires, as a result of partial suppression of superconductivity in regions near the domain walls. In our system, an  $\text{Al}_2\text{O}_3$  insulating barrier is present between the ferromagnet and the superconductor, which prevents direct electronic communication between the layers, precluding proximity effects and spin accumulation. This implies that the stray magnetic fields are the origin of the observed magnetoresistance in this particular system.

The narrow strips were fabricated by depositing the layers onto Si substrates with pre-patterned electron-beam resist, followed by liftoff processes. A scanning electron microscope (SEM) image of an actual device is shown in Fig. 1(a). The sample stack is (thicknesses in nm): 3 Cr/6  $\text{Ni}_{80}\text{Fe}_{20}$ /1  $\text{Al}_2\text{O}_3$ /20 Al/0.7  $\text{Al}_2\text{O}_3$ /3 Cr/5 Au. A 1 nm  $\text{Al}_2\text{O}_3$  layer was introduced between the NiFe and Al layers in order to suppress the proximity effect and to maintain a suitable  $T_C$ .<sup>22</sup> Another 0.7 nm  $\text{Al}_2\text{O}_3$  placed above the Al layer cuts down the proximity influence from the top electrode while still allowing good electrical contacts from the top. The wire width was 1  $\mu\text{m}$  and the length between the contacts was 13  $\mu\text{m}$ . The wire contained double-notches  $\sim 250$  nm deep (forming narrow constrictions with  $\sim 500$  nm width) placed 1  $\mu\text{m}$  apart. The samples were deposited onto liquid nitrogen cooled substrates through thermal and electron-beam evaporation at a system base pressure of  $6 \times 10^{-8}$  Torr. Electrical contacts of 5 Cr/40 Cu (in nm) were formed by magnetron sputtering after a second step electron-beam lithography. The transport measurement was performed using a standard four terminal method with a fixed dc current of 10  $\mu\text{A}$ , and the samples were fully submerged in a pumped liquid He<sup>4</sup> reservoir during the measurements with precise temperature control ( $\pm 2$  mK) achieved by varying the vapor pressure above the liquid.

The principle of operation in these devices is illustrated in Fig. 1(b). When the wire is magnetically saturated in the negative direction and held below the superconducting

<sup>a)</sup>Author to whom correspondence should be addressed. Electronic mail: gxmiao@mit.edu.

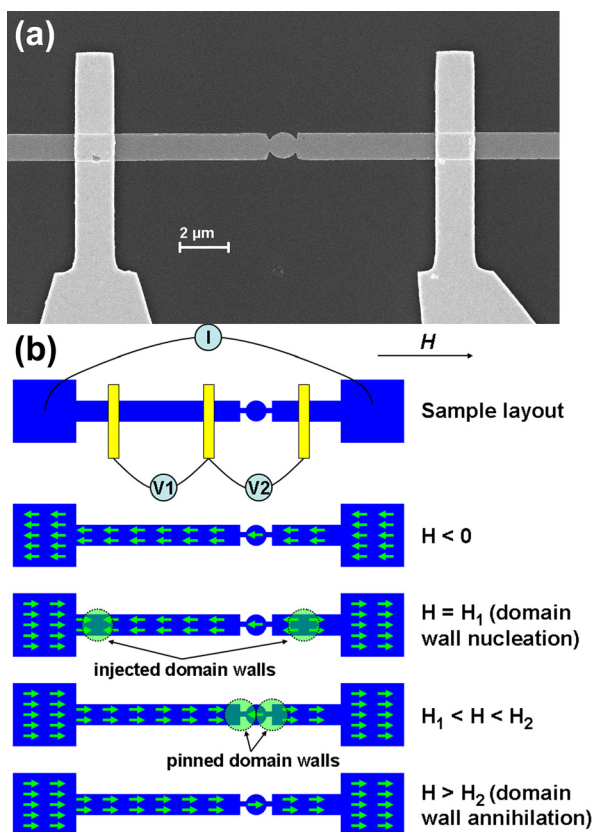


FIG. 1. (Color online) (a) SEM image of a notched device. The nominal wire width and the distance between the notches are both  $1 \mu\text{m}$ , and the notch depth is about  $250 \text{ nm}$ . The distance between the two voltage leads is  $13 \mu\text{m}$ . (b) Schematic of the sample layout and its principle of operation. V1 and V2 are voltmeters to record the signals from the control device and the notched device simultaneously. The expected magnetization directions are marked with arrows and the domain wall positions with circles.

critical temperature, the system is in a low resistance state. As the applied magnetic field increases in the positive direction to a field  $H_1$ , two domain walls are injected from the pads at the ends of the wire and traverse the wire until they reach the notched region, where they are pinned. The stray fields from the walls locally destroy the superconductivity and the system goes into a stable higher resistance state. The domain wall velocity in NiFe wires can reach hundreds of  $\text{m/s}$  (Ref. 23) and is too fast to detect in the dc measurements. When the applied field reaches  $H_2$ , it is sufficient to unpin the domain walls from the notches and saturate the wire, and the system returns to the low resistance state.

Figure 2 shows the resistance as a function of applied magnetic field for one device with notches, and a control device without any notches (black data points) which was fabricated and measured simultaneously. The wire resistance is about  $44 \Omega$  in its normal state. Near the superconducting transition temperature, a large MR develops in the notched wires. On the other hand, the control device does not show any noticeable magnetoresistance (random sharp spikes arise from dynamic electronics response due to the series connection), confirming that the observed MR indeed originates from contributions of the pinned domain walls. The domain walls were injected at a field of  $25\text{--}30 \text{ Oe}$  and typically annihilated by about  $50 \text{ Oe}$ .

To quantify the domain wall stray field, the object oriented micromagnetic framework (OOMMF) code was used to calculate the magnetization and the stray field distributions

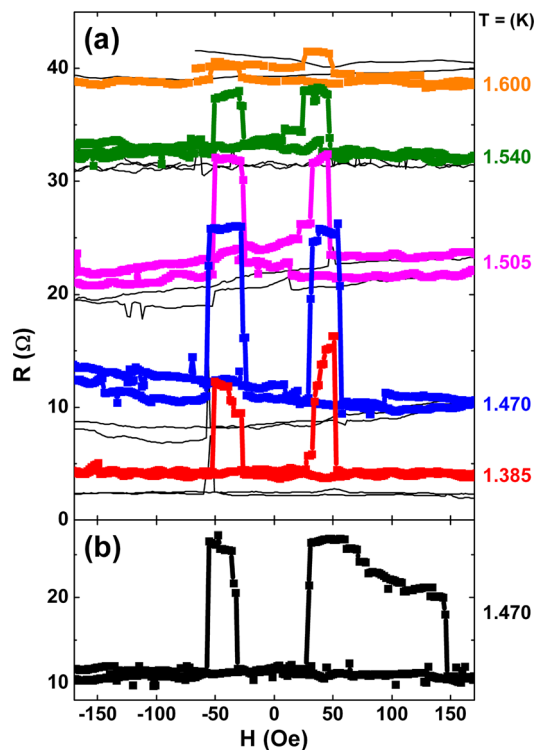


FIG. 2. (Color online) (a) Device resistance as a function of the applied field. The corresponding measurement temperatures are labeled on the right side. Colored curves are from the notched device while the black curves are from the accompanying control device. The two sets of data were recorded simultaneously at each temperature. (b) An example of the presence of a significantly higher switching field  $H_2$  in the ascending branch of a cycle measured at  $1.47 \text{ K}$ .

around a model of the wire. The simulation was based on the actual shape of the device taken from a SEM image, into which two  $180^\circ$  domain walls were placed and allowed to equilibrate at remanence. The simulation was carried out with an in-plane cell size of  $4 \text{ nm}$  and a cell size of  $2 \text{ nm}$  in the out-of-plane direction and used standard parameters for NiFe. The model shows that the walls are transverse in type and have a core region that is magnetized perpendicular to the wire length. The cores of the two walls can be oriented parallel or antiparallel. Fig. 3(a) illustrates the magnetization distribution in the case where the cores are parallel, which is the expected configuration if there is any misalignment between the field direction and the length of the wire leading to an in-plane field component perpendicular to the wire. Figs. 3(b) and 3(c) illustrate the stray field produced by the pinned domain walls, showing the out-of-plane and in-plane field magnitude at a height of  $14 \text{ nm}$  above the mid-thickness of the NiFe layer, corresponding to mid-thickness of the Al layer, i.e., the calculated field strength approximates the average field inside the Al layer.

The stray field from the domain walls has its most dramatic effect at temperatures in the range of  $1.38$  to  $1.6 \text{ K}$ , close to  $T_C$ , where the superconductivity is most vulnerable to magnetic fields. The maximum observed resistance change is as large as  $15 \Omega$  or  $35\%$  of the normal state resistance. This is equivalent to suppressing superconductivity over a  $4.5 \mu\text{m}$  long portion of the wire. The behavior of the critical field in thin Al films is well documented.<sup>24</sup> The in-plane critical field  $H_C$  for a  $20 \text{ nm}$  thick Al film is around  $6 \text{ kOe}$  at  $0.4 \text{ K}$ , much larger than its bulk value ( $100 \text{ Oe}$ ) because of the thin film geometry.



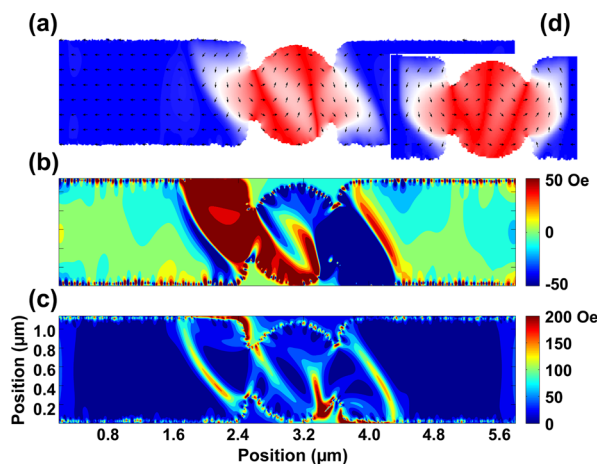


FIG. 3. (Color online) (a) Simulation of the remanent magnetic configuration of two trapped  $180^\circ$  domain walls in the notched sample, for the case where the cores of the walls are parallel. (b) The out-of-plane and (c) the in-plane magnetic field magnitude at a height corresponding to mid-thickness of the Al superconductor film. (d) The remanent magnetization configuration for the case where the cores of the  $180^\circ$  domain walls are antiparallel. The  $x$  and  $y$  directions of the above figures correspond to the actual lateral dimensions of the device, and the colors map out the magnetic field intensity.

We can make an order of magnitude estimate of the value of  $H_C$  in the devices in order to compare with the stray field from the domain walls. Fig. 2 suggests that  $T_C$  is around 1.5 K in the device. For thin films, the in-plane  $H_C$  varies as  $\sqrt{1 - T/T_C}$  with temperature. This means that, for the temperatures examined in this experiment, for example 1.47 K,  $H_C$  is still on the order of 1 kOe for an in-plane field, while only about 50 Oe for an out-of-plane field (lowered by a factor of  $\xi(T)/d$  due to geometrical reasons).<sup>24</sup> The out-of-plane critical field in particular is modest compared to the stray fields that are present near a domain wall in a NiFe film. Fig. 3(b) shows that the out-of-plane component of the stray field exceeds  $\sim 50$  Oe over a distance of about  $3 \mu\text{m}$ . Because of the spatial extent of the Cooper pairs ( $\xi \sim 400$  nm with the above parameters, significantly shorter than the bulk superconducting coherence length of 1200 nm because the electron mean free path is also limited by the film thickness  $d$ ), the stray fields can suppress superconductivity in a region greater than this  $3 \mu\text{m}$  length. This result is consistent with the estimated length over which superconductivity is suppressed in the presence of the domain walls. On the other hand, the in-plane field component (Fig. 3(c)) is not strong enough to induce significant change of superconductivity (and hence resistance) in these devices.

The OOMMF simulations show that the stray fields are not only present at the notched area, but they also appear at the wire edges due to edge roughness. These fields can suppress superconductivity near the edges of the wires, leading to a reduction in  $T_C$  with wire width. This is supported by measurements on 500 nm wide wires, for which the  $T_C$  was below 1 K, the limit of temperature control of the experimental apparatus. This edge effect is independent of the presence of domain walls hence is not expected to contribute to the observed magnetoresistance. Similarly, any stray fields originating from film roughness also would not contribute to the magnetoresistance.

Finally, it is interesting to consider the case in which the cores of the domain walls are antiparallel. The injected walls form a structure analogous to a  $360^\circ$  domain wall at the

notches, which is magnetostatically stabilized and is more difficult to annihilate.<sup>25</sup> During multiple field cycles, we did occasionally (once in  $\sim 30$  cycles) observe the high resistance state persisting to a significantly higher field of over 150 Oe. An example of this is shown in the ascending branch of Fig. 2(b). It is notable that the resistance drops gradually before the reversal is completed, which may be a result of compression of the coupled pair of domain walls by the field prior to annihilation.

In summary, the injection and annihilation of magnetic domain walls was used to induce a large magnetoresistance in Al/alumina/NiFe wires held near the superconducting critical temperature. The stray fields generated by the domain walls in the NiFe penetrate the superconducting film and drive it towards its normal state, leading to a large positive MR. The possibility of using controllable domain wall motion to manipulate superconductivity makes it plausible to combine the advantages of superconductor- and domain-wall-based devices with simultaneous control by temperature and field, for future spintronic as well as quantum computing applications.

Support from the NRI INDEX Program and NSF DMR 0504158 are gratefully acknowledged.

- <sup>1</sup>L. R. Tagirov, *Phys. Rev. Lett.* **83**, 2058 (1999).
- <sup>2</sup>A. I. Buzdin, A. V. Vedyayev, and N. V. Ryzhanova, *Europhys. Lett.* **48**, 686 (1999).
- <sup>3</sup>C. H. Bennett and D. P. DiVincenzo, *Nature* **404**, 247 (2000).
- <sup>4</sup>P. Recher, E. V. Sukhorukov, and D. Loss, *Phys. Rev. B* **63**, 165314 (2001).
- <sup>5</sup>J. D. Sau, R. M. Lutchyn, S. Tewari, S. Das Dharma, *Phys. Rev. Lett.* **104**, 040502 (2010).
- <sup>6</sup>A. C. Potter and P. A. Lee, *Phys. Rev. Lett.* **105**, 227003 (2010).
- <sup>7</sup>A. I. Buzdin, *Rev. Mod. Phys.* **77**, 935 (2005).
- <sup>8</sup>F. S. Bergeret, A. F. Volkov, and K. B. Efetov, *Rev. Mod. Phys.* **77**, 1321 (2005).
- <sup>9</sup>A. Yu Aladyskhin, A. V. Silhanek, W. Gillijns, and V. V. Moshchalkov, *Supercond. Sci. Technol.* **22**, 053001 (2009).
- <sup>10</sup>J. Y. Gu, C. Y. You, J. S. Jiang, J. Pearson, Ya. B. Bazaliy, and S. D. Bader, *Phys. Rev. Lett.* **89**, 267001 (2002).
- <sup>11</sup>I. C. Moraru, W. P. Pratt, and N. O. Birge, *Phys. Rev. Lett.* **96**, 037004 (2006).
- <sup>12</sup>C. Visani, V. Pena, J. Garcia-Barriocanal, D. Arias, Z. Sefrioui, C. Leon, and J. Santamaria, *Phys. Rev. B* **75**, 054501 (2007).
- <sup>13</sup>G. X. Miao, A. V. Ramos, and J. S. Moodera, *Phys. Rev. Lett.* **101**, 137001 (2008).
- <sup>14</sup>V. Pena, Z. Sefrioui, D. Arias, C. Leon, J. Santamaria, J. L. Martinez, S. G. E. te Velthuis, and A. Hoffmann, *Phys. Rev. Lett.* **94**, 057002 (2005).
- <sup>15</sup>A. Y. Rusanov, S. Habraken, and J. Aarts, *Phys. Rev. B* **73**, 060505 (2006).
- <sup>16</sup>A. Singh, C. Surgers, R. Hoffmann, H. Lohneisen, T. V. Ashworth, N. Pilet, and H. J. Hug, *Appl. Phys. Lett.* **91**, 152504 (2007).
- <sup>17</sup>Z. R. Yang, M. Lange, A. Volodin, R. Szymczak, and V. V. Moshchalkov, *Nature Mater.* **3**, 793 (2004).
- <sup>18</sup>A. Y. Rusanov, T. E. Golikova, and S. V. Egorov, *JETP Lett.* **87**, 175 (2008).
- <sup>19</sup>L. Y. Zhu, T. Y. Chen, and C. L. Chien, *Phys. Rev. Lett.* **101**, 017004 (2008).
- <sup>20</sup>J. Zhu, X. Cheng, C. Boone, and I. N. Krivorotov, *Phys. Rev. Lett.* **103**, 027004 (2009).
- <sup>21</sup>J. E. Villegas and I. K. Schuller, *Supercond. Sci. Technol.* **24**, 024004 (2011).
- <sup>22</sup>G. X. Miao, K. S. Yoon, T. S. Santos, and J. S. Moodera, *Phys. Rev. Lett.* **98**, 267001 (2007).
- <sup>23</sup>M. Hayashi, L. Thomas, C. Rettner, R. Moriya, Y. B. Bazaliy, and S. S. P. Parkin, *Phys. Rev. Lett.* **98**, 037204 (2007).
- <sup>24</sup>R. Meservey and P. M. Tedrow, *Phys. Rep.* **238**, 173 (1994).
- <sup>25</sup>F. J. Castano, C. A. Ross, C. Frandsen, A. Eilez, D. Gil, H. I. Smith, M. Redjidal, and F. B. Humphrey, *Phys. Rev. B* **67**, 184425 (2003).